Investigation into the transportation and melting of thick ice slurries in pipes

T.S. Evans, G.L. Quarini, G.S.F. Shire

Department of Mechanical Engineering, University of Bristol,

Queen's Building, University Walk, Bristol BS8 1TR, UK

Abstract

This paper presents the results of experiments and modelling carried out on ice slurries flowing in uninsulated steel pipes with a nominal diameter of 50 mm. The slurries used were formed from 4.75% NaCl aqueous solution and had ice mass fractions in the range 18–42%, with a view to the use of thick ice slurry 'pigs' as a pipeline clearing technique. Of particular interest was the distance over which such slurries can survive as plug-like entities, before melting reduces them to ineffective thin two-phase suspensions. The experiments showed that for small volumes of slurry, survivability is directly proportional to the quantity of slurry used, but that increasing the ice fraction has a more marked effect. A simple one-dimensional numerical model that accounts for transportation, heat transfer and melting was developed that produces reasonable predictions.

Keywords:

Ice slurry, Melting, Heat transfer, Cooling, Pipe, Flow

Nomenclature

C	mass concentration of freezing point depressant
c_p	specific heat capacity (J kg^{-1} K^{-1})
D	diffusivity (m^2 s^{-1})
h	heat transfer coefficient (W m^{-2} K^{-1})
k	thermal conductivity (W m^{-1} K^{-1})
l	initial length (m)
L	survival distance (m)
Nu	Nusselt number
Pr	Prandtl number
Re	Reynolds number
r	radius (m)
T, ΔT	temperature (K)
t, Δt	time (s)
U	U-value (W m^{-2} K^{-1})
u	velocity (m s^{-1})
x	position (m)

Greek

α	coefficient (K)
η	viscosity (Pa s)
λ	latent heat of fusion (J kg^{-1})

ρ	density (kg m^{-3})
ϕ	ice fraction
ϕ'	relative ice fraction

Subscripts

air	air
app	apparent
e	environment
b	brine
I	inner
i	ice
ifp	initial freezing point
ffp	final (eutectic) freezing point
m	mass
max	maximum packing
O	outer
p	pipe wall
s	slurry
v	volume
w	water

---

1. Introduction

The majority of existing literature on ice slurries focuses on the knowledge required for applications in cooling (Kauffeld et al., 2005; Bellas and Tassou, 2005; Davies, 2005), typically with a view to replacing existing single-phase secondary refrigerants. One of the potential benefits is a reduction in capital costs associated with the downsizing of distribution networks (Metz and Margen, 1987); this is possible because of the high effective heat capacity of ice slurry compared to non-phase-changing heat transfer fluids, along with the potential for improved heat transfer (Bellas et al., 2002). However, in order to ensure that pumping energy costs do not outstrip the savings made, the tendency is to employ slurries with a relatively low ice (solid) fraction.

It is generally recognised that at a certain ice fraction, the pressure drop in a flowing ice slurry becomes significantly elevated relative to water. Researchers differ in the values they attribute, both for the shift away from Newtonian behaviour, and the upper limit for a viable refrigerant. In their 2002 review paper, Ayel et al. (2002) note that the reported cut-off for Newton behaviour in ice slurries varies between 6% and 15%, with Bingham models favoured thereafter. In practice it appears that most experiments in the field adopt ice fractions of no more than 25–30%. In addition to ensuring a workable pressure drop, other reasons for limiting the ice content include the need for good heat transfer properties (Niezgoda-Zelasko, 2006) and guarding against the formation of blockages (Hansen et al., 2002).

1.1. Ice pigging

In contrast to refrigeration, ‘ice pigging’ requires the use of significantly higher ice fractions to obtain the desired flow behaviour. This patented method of clearing complex pipelines (Quarini,

2001) has been pioneered by the University of Bristol and relies on the use of thick ice slurries to create deformable plugs, dubbed ‘ice pigs’. Shire et al. (2005b) have shown that by introducing an ice slurry with sufficiently high ice fraction to a duct, a plug is formed that tends to maintain itself against mixing whilst being driven by a differential pressure, even through relatively complex topologies. It is thus able to negotiate pipework that would be inaccessible to the types of solid pigs originally developed for the hydrocarbons industry. A study of the pressure drops encountered in ice pigging was reported recently by Shire (2006).

Tests on the performance of ice pigs were carried out by Quarini (2002), who demonstrated that they could be used for:

- removing soft fouling and deposits from a pipe;
- recovering product from a pipe at the end of a production run; and
- separating different batches of products flowing through the same pipe.

Products successfully tested by the authors have included foods (e.g. sauces, fats, and pastes), pharmaceuticals and paints, and the removal of particulates from potable water pipes has also been trialled. Ice pigging can reduce waste and offers savings of chemicals and effluent treatment compared to traditional clean-in-place (CIP) methods employed in the process industries.

The melting of the ice is a beneficial fail-safe feature of an ice pig, but is also the principal limiting factor for its useful lifetime. High ice fraction slurries are thus favoured not only for their plug-flow characteristics, but also because of their ability to absorb more heat before

becoming unfit for purpose. In this paper the authors present a simple numerical model for predicting the distance over which a slug of ice slurry is able to perform pigging duties, backed-up with experimental results.

It is considered that as well as being of direct relevance in the application of ice pigging, the work will also be of interest to the wider ice slurry community, by presenting results on ice slurries with higher solid fractions than have generally been reported.

2. Model for ice pig survivability

A relatively quick and simple method was sought for predicting the temperature and the ice fraction of a slurry moving through a pipe as a function of time.

2.1. Arrangement

The model considers a continuous cylindrical pipe with inner and outer radii r_I and r_O, respectively, surrounded by air at constant temperature, T_e. Fluid flows through the pipe at a velocity u and is characterised by a temperature T and an ice fraction ϕ_m. A simplification is made whereby the system is taken to be one-dimensional, i.e. a single chain of cells, such that the parameter values are averaged over the entire cell. Since the ice slurry adopts a plug-flow nature, axial mixing due to velocity gradients can be disregarded.

The governing equation for ice fraction is:

$$\left(\frac{\partial \phi_m}{\partial t} + u\frac{\partial \phi_m}{\partial x}\right) = \left(\frac{\partial}{\partial x} D \frac{\partial \phi_m}{\partial x}\right) - \frac{2U_I}{\rho_s \lambda r_I}\left(T_p - T\right) \quad (1)$$

where f m is the mass fraction of ice, t is time, x is the spatial co-ordinate, D is the diffusivity coefficient, U_I is the U-value between pipe and fluid, ρ_s is the overall fluid density, λ is the latent heat of fusion, and T_p is the pipe wall temperature.

Overall density r s is given by:

$$\rho_s = \frac{1}{\frac{\phi_m}{\rho_i} + \frac{1-\phi_m}{\rho_b}} \tag{2}$$

where ρ_i and ρ_b are the densities of ice and brine. Since the concentrated suspension is advection-dominated, diffusion between the phases is neglected and so D→0. For simplicity U_I assumes water at 20 °C:

$$\frac{1}{U_I} = \frac{2r_I}{k_w Nu} + \frac{\frac{1}{2}(r_o - r_i)}{k_p} \tag{3}$$

where k_w and k_p are the thermal conductivities of water and the pipe wall, and the Nusselt number is given by the Dittus–Boelter equation:

$$Nu = 0.023 Re^{0.8} Pr^{0.33} \tag{4}$$

with Reynolds number:

$$Re = \rho_w \, u \, 2r_I / \eta_w \tag{5}$$

and Prandtl number:

$$Pr = \eta_w \, c_p / k_w \tag{6}$$

where ρ_w , η_w and $c_{p,w}$ are the density, viscosity and specific heat capacity of water.

The governing equation for fluid temperature T is:

$$\overline{\rho c_p}\left(\frac{\partial T}{\partial t}+u\frac{\partial T}{\partial x}\right)=\left(\frac{\partial}{\partial x}k\frac{\partial T}{\partial x}\right)+\frac{2U_I}{r_I}\left(T_p-T\right) \tag{7}$$

where ρc_p is the volumetric heat capacity of the fluid and k is the thermal conductivity (both of which are calculated as weighted means of the values for each phase).

The governing equation for pipe wall temperature T p is:

$$\left(\rho c_p\right)_p\frac{\partial T_p}{\partial t}=k\frac{\partial^2 T}{\partial x^2}+\frac{2}{\left(r_O^2-r_I^2\right)}\left(r_O U_O\left(T_e-T_p\right)-r_I U_I\left(T_p-T\right)\right) \tag{8}$$

where $(\rho c_p)_p$ and k_p are the volumetric heat capacity and the thermal conductivity of the pipe wall, and U_O is the U-value between the environment and the pipe wall:

$$\frac{1}{U_O}=\frac{1}{h_{air}}+\frac{\frac{1}{2}\left(r_O-r_I\right)}{k_p} \tag{9}$$

where h_{air} = 20 W m^{-2} K^{-1} for stainless steel in air.

In order to maintain the relationship between T and f m , the following equation is applied:

$$\phi_m=\begin{cases}0, & T>T_{ifp}\\ \left(\dfrac{T-T_{ifp}}{T_{ffp}-T_{ifp}}\right), & T_{ffp}<T<T_{ifp}\end{cases} \tag{10}$$

where T_{ifp} and T_{ffp} are the initial freezing and the final freezing (eutectic) temperatures of the slurry. For the NaCl + H_2O system, T_{ifp} is given a first-order approximation:

$$T_{ifp} = T(0) - \alpha C, \qquad 0 < C < 0.2 \tag{11}$$

where C is the bulk salt concentration, α = 100 K and $T(0)$ = 273.15 K. The dependence of T on ϕ_m and C laid-out by Eqs. (10) and (11) is evidently a crude simplification; however, it is only used to adjust the bulk fluid temperature for a given ice fraction. Whilst this results in some inaccuracies in T (and hence heat flux), the impact on the evolution of ice fraction with time is considered to be relatively small.

2.2. Numerical solution

A program has been written in Visual Basic that solves Eqs. (1), (7) and (8) numerically using the Thomas–Gauss tridiagonal matrix method, then adjusts T using Eq. (10) to restore the ice–water equilibrium. The non-linearity introduced by terms containing two variables is dealt with by using values from the previous time-step; the error thus introduced diminishes as Dt/0. Survival distance L is defined for this study as being the distance a slug of ice slurry travels before it drops below the threshold quality; this is chosen as being at least a 2 m length where ϕ_m > 8%. These properties are dictated more by the detection capabilities of the instruments than suitability for ice pigging applications.

3. Experiments

3.1. Ice generation

A Ziegra scraped surface ice maker is used to produce ice slurry from a brine containing a mass concentration of 4.75% NaCl. Production continues until the receiving tank contains a sufficient quantity of slurry at approximately the desired ice fraction, which (optionally) can be adjusted with the addition or removal of brine.

3.2. Ice fraction measurement

A simple batch technique is employed to estimate the ice volume fraction manually, using a coffee press (i.e. a mesh plunger) to separate the solid and liquid fractions of a slurry sample held in a beaker. The volumes of the two components allow a relative ice volume fraction ϕ'_v to be calculated using the equation:

$$\phi'_v = \frac{V_{i,app}}{V_s} \tag{12}$$

where $V_{i,app}$ is the apparent volume of compacted ice crystals and V_s is the total volume of slurry. Note that ϕ'_v is the ratio ϕ_v / $\phi_{v,max}$ where ϕ_v is the true volumetric ice fraction and $\phi_{v,max}$ is the maximum packing fraction. This technique is especially useful for field work, since it provides a practical measurement that can be made without sophisticated instrumentation. Furthermore, ϕ'_v is itself an important parameter for characterising the flow behaviour of a slurry (e.g. Mooney, 1951).

To compare experimental and numerical data, a value for the maximum packing factor is required. Close-packed monodisperse spheres have $\phi_{v,max}$ = 74%, but examinations of ice slurries have indicated a more prolate crystal form, such as ellipsoids (Hansen et al., 2002) with $\phi_{v,max}$ up to 76% (Wills, 1991), or spherocylinders (Sari et al., 2000) with $\phi_{v,max}$ up to 91% (Donev et al., 2004). Under real conditions a polydisperse system will tend to increase the maximum packing factor, although disordered packing has the opposite effect.

A calibration of the coffee press technique was carried out using two methods: firstly a phase balance calculation using *T* and *C*, and secondly a batch hot water calorimetry procedure similar to that described by Stamatiou et al. (2002). These resulted in values for f m that agreed within ±5% and gave $\phi_{v,max}$ = (60 ± 4)%.

The conversion between volume and mass fractions requires the equation:

$$\phi_m = \phi_v \frac{\rho_i}{\rho_s} \tag{13}$$

3.3. Test loop

The test loop is part of a larger experimental facility designed to mimic the pipework found in many food factories (see Fig. 1). It is constructed mainly from 316L stainless steel pipe of nominal 50 mm diameter, but also includes four lengths of reinforced clear PVC tubing to facilitate visual observations. Apart from the ice storage tank the rig is not insulated.

Fig. 1 – Ice pigging test facility at the University of Bristol.

Ice slurry is delivered from a manually stirred 40 l hopper mounted above a lobe pump; there is also a supply of mains water. A variable speed single stage centrifugal pump allows fluid to be circulated around the loop, which is approximately 56 l (equivalent to 31 m). Although Fig. 2 depicts a simple topology, the experimental rig actually includes 30 right-angle bends, 12 instrument stubs, and several expansions and contractions.

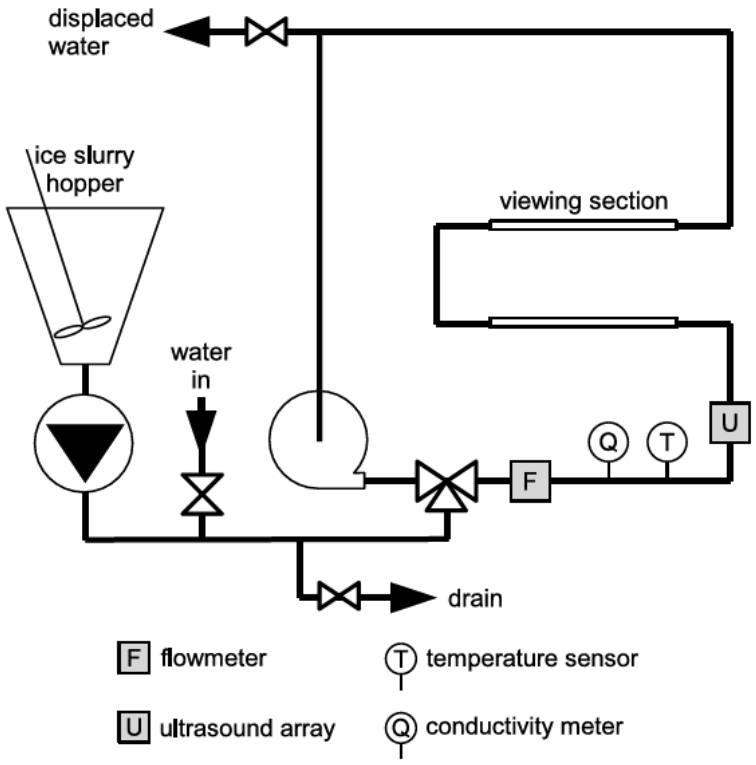

Fig. 2 – Simplified diagram of the experimental rig.

The instrumentation comprises an electromagnetic volume flowmeter, a conductivity meter and two Pt100 temperature sensors. Data logging is performed in Matlab via an analogue-to-digital

converter at a frequency of 2 s^{-1}. Further measurements of the system are made with the use of an in-house ultrasound sensor arrangement, described by Shire et al. (2005a). A pair of ultrasonic transducers is clamped on opposing sides of the pipe, one of which is fired repeatedly whilst the other picks up the transmitted signal. The received amplitude is logged and used to detect the presence of ice crystals.

3.4. Procedure

Prior to an experiment, the test loop is filled with water at ambient temperature and is de-aerated. After measuring ϕ'_v, ice slurry is pumped into the insertion pipe, displacing air to the drain. The insertion valve is then opened and ice slurry enters the test loop, displacing water from the upper valve. Once the required volume has been pumped in, the valves are switched, closing the loop. The circulation pump is switched on, driving the water and ice slurry around the loop until all ice have been melted, as confirmed by temperature and ultrasound data.

3.5. Data analysis

Preliminary tests were used to build-up a framework for assessing the integrity and survival distance of an ice pig. Visual and aural observations allowed an estimate to be made of the number of circuits completed, which then informed analysis of the logged data. It was found that whilst T and C are useful location markers, they are unable to give direct measurements of the ice fraction within the pipe. Aside from the response times of the instruments, this is mainly due to the transient nature of the tests. Heat gains, along with mixing of the ice slurry with the leading/trailing water, mean that conditions change too quickly to permit an equilibrium between phases to be maintained after insertion. Instead, as stated in Section 2.2, a threshold amplitude of

15 mV was chosen for the received ultrasound signal, below which the pipe was taken to contain fluid with $\phi'_v < 15\%$.

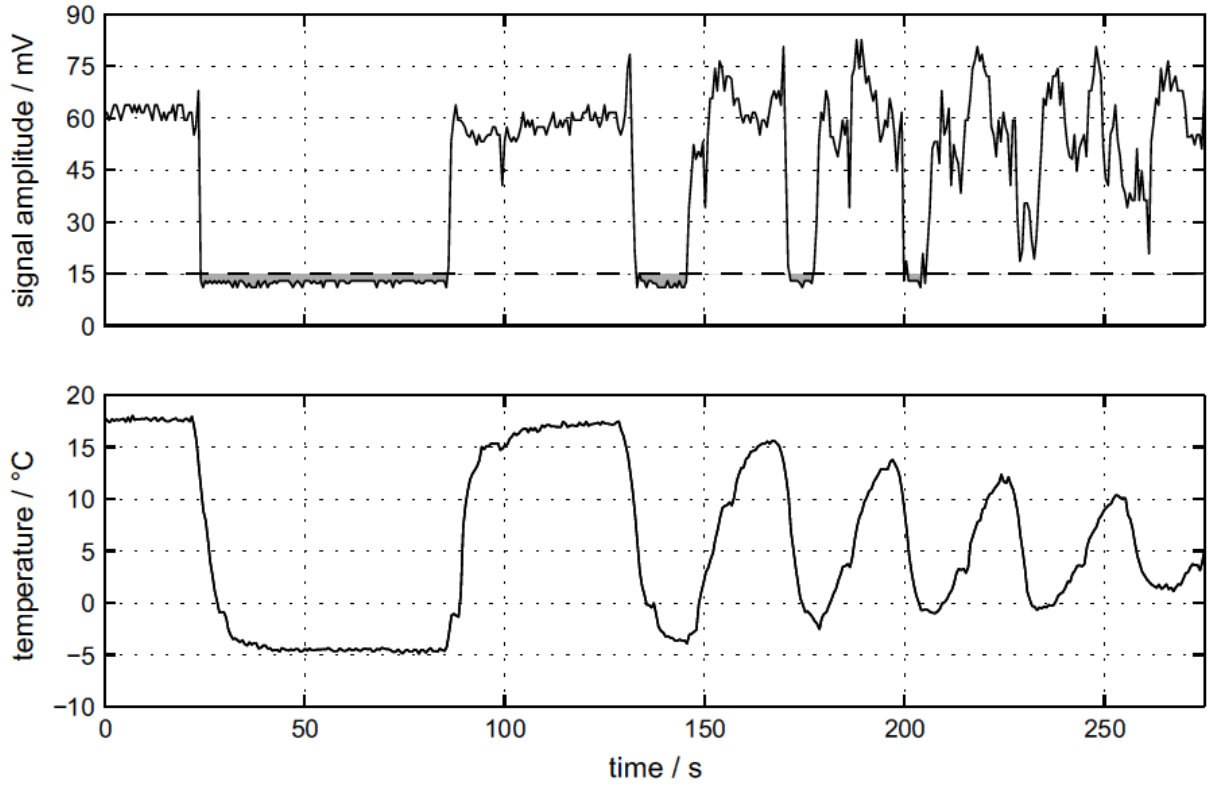

Fig. 3 – Typical experimental data, with received ultrasound amplitude (top) and temperature (bottom) plotted against time. The shaded regions in the upper plot show where the ultrasound signal has dropped below the threshold value, thus flagging the detection of ice slurry with $\phi'_v > 15\%$.

Fig. 3 depicts a representative set of experimental data, in which V_s = 17 l (l = 9.5 m), ϕ_m = 38% (ϕ'_v = 70%) and u = 1 m s^{-1}. In this example, the slurry is pumped into the system during 20 s < t < 80 s, after which the circulation pump is started immediately, achieving full velocity at around t = 120 s. The cyclic nature is evident with a period ≈30 s, with the last threshold-

crossing ultrasound signal occurring at t = 210 s indicating that the ice pig survived for approximately three circuits. Interpolation of the data permits a more precise estimate of the survival distance as L = (104 ± 10) m.

4. Results and discussion

4.1. Varying length of ice pig

It was clear that increasing the volume of slurry would extend the distance it could be pumped before becoming unviable as an ice pig. A simple prediction was that there might be a simple proportionality, but the exact relationship was not known. An initial approximation would be to equate the sensible heat from the pipe wall to the latent heat of the ice, with $\Delta T = (T_p - T)$. As Fig. 4 shows, the model does indeed predict a fairly linear dependence (with a small tail for $l \leq 2$ m caused by the choice of validity criteria). This is reasonable when it is considered that the ice slurry is continuously being presented with pipe walls at the ambient temperature, leading to a constant melting rate. However, when looking at the large scale predictions shown in Fig. 5 it is evident that the survival distance begins to tail-off as l increases. This can be attributed to the increasing influence of heat transfer from the environment to ice slurry through the pipe walls, and suggests that there is a finite limit to L.

The experimental results presented in Fig. 4 are in good numerical agreement with the model, albeit with a rising trend for longer ice pigs. A possible explanation for this feature arises from the fact that the tests are performed on a loop rather than a continuous pipe, which was a practical necessity. When the volume of the ice pig tends towards the volume of the loop, the amount of warm water available to maintain the pipe wall temperature tends to zero. Essentially

the thermal memory of the pipe, caused by the low rate of heat transfer from the surrounding air, means that less heat is being put into melting the ice.

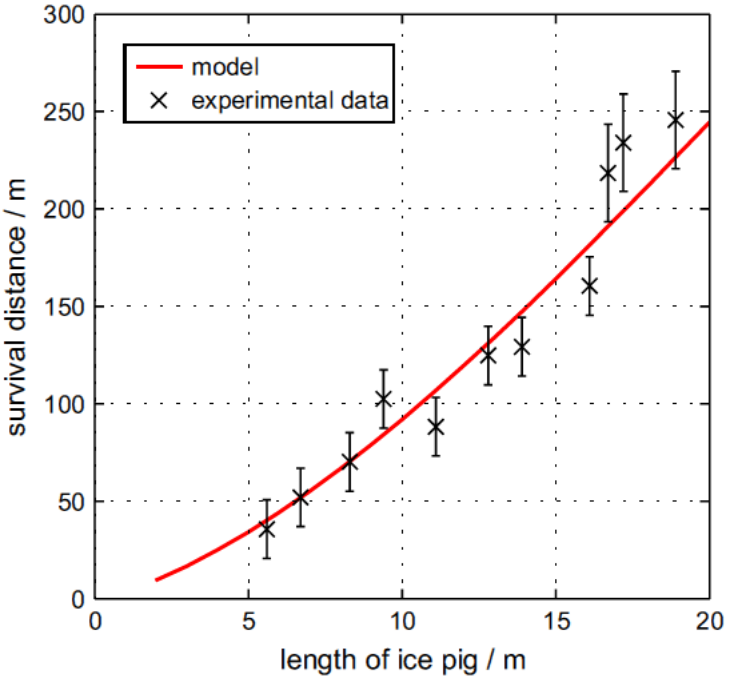

Fig. 4 – Plot of survival distance against ice pig length, with ϕ'_v [70% (comparison of experimental and model data).

Because the model neglects the repeated passes through a high shear pump, two factors that are detrimental to survivability are ignored: forced mixing of the warm water with the ice slurry, and mechanical heat gains. Again this is an artefact of the loop set-up, so would be less significant in a real life implementation (particularly if a positive displacement pump was employed).

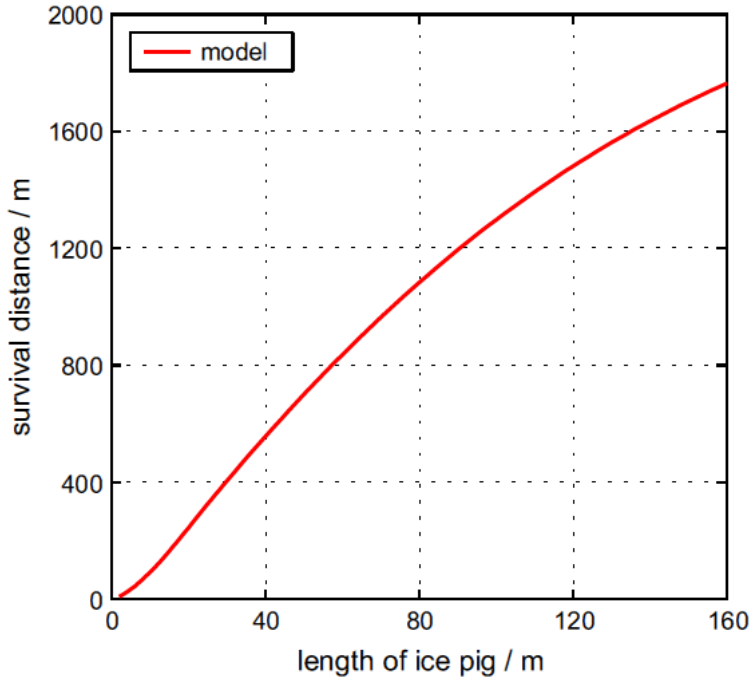

Fig. 5 – Plot of survival distance against ice pig length, with ϕ'_v [70% (extended model data).

4.2. Varying solid fraction of ice pig

The effect of varying ice fraction on survival distance is less obvious than the previous case, although it is clear that for a given volume of slurry, L will increase with ϕ. This is because the heating rate is fixed by the ice pig length and the temperature difference, which is fairly insensitive to the ice fraction. (Similar logic suggests that a higher u will also increase L, but this is beyond the scope of the present study.) As Fig. 6 indicates, the model predicts a virtually straight-line relationship, with a slight deviation near the minimum ϕ threshold.

One of the initial predictions was that higher values of ϕ might result in significantly greater L due to the flow behaviour of very stiff slurries. Because of the assumptions made by the model about heat transfer and flow behaviour, this trait is not evident in the simulated data. However,

the experiments do seem to show a higher-order relationship between ϕ and L, particularly for $\phi_m \geq 38\%$ ($\phi'_v \geq 69\%$). This suggests that the survival distance of an ice pig can be extended by partial dewatering, i.e. L is dependent on more than simply the initial mass of ice. General experience has shown that these high ϕ slurries are indeed particularly effective for ice pigging, both in respect of their flow behaviour and longevity.

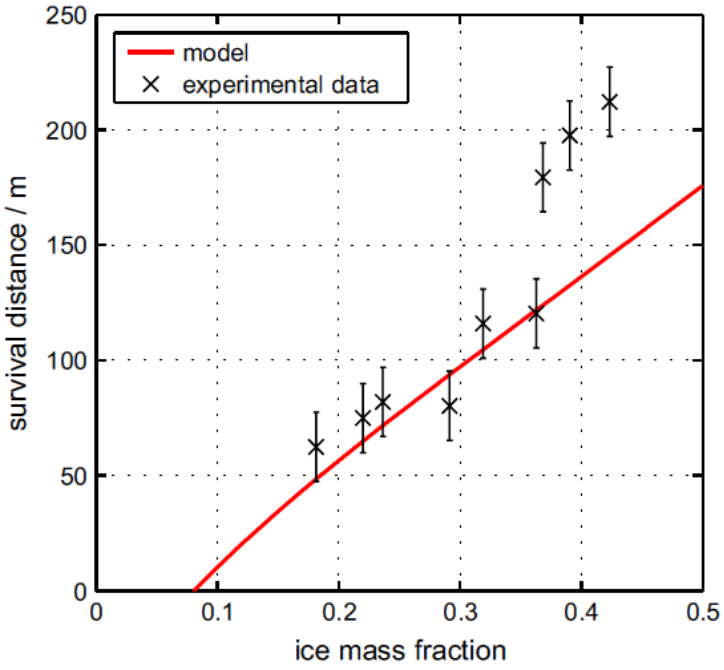

Fig. 6 – Plot of survival distance against ice fraction, with l [13 m (comparison of experimental and model data).

As observed in Section 4.1, the experimental survival distances are generally slightly higher than the model predicts; however, L apparently levels-off as $\phi \rightarrow 0$. It is proposed that this discrepancy is caused by the limited instrumentation on the test loop, which makes accurate interpolation of L difficult when the number of completed circuits is small. There were also unavoidable differences in the ice quality assessment criteria between the experiments and the simulations.

5. Future work

This study has indicated further useful work that could be carried out along a similar vein.

- As alluded to in Section 4.2, the effect of flow velocity could be studied. Experiments could be conducted to test the predictions of the model for large values of *l*.
- The model may be extended to allow for the pipe having thick walls, or being surrounded by a solid/liquid instead of air. The modelled geometry could also be altered to permit a core plug-flow region and a circumferential laminar-flow region, which would better reflect the velocity profile found by researchers such as Sari et al. (2000).
- Increasing the complexity of the model with more accurate equations for ice fraction, viscosity and heat transfer would allow for better agreement with the experimental data. Other physical behaviour that could be considered includes inter-phase slip, melting kinetics and internal dissipation.

6. Conclusions

The melting behaviour in flowing plugs of thick ice slurry has been studied numerically and experimentally, to ascertain the distance over which they can survive as useful entities. Survival distance L increases with increasing ice fraction f and starting length *l*, in line with expectations. The numerical model predicts a first-order dependence of *L* for low *l*, tending towards an asymptotic limit as *l* increases. When varying ϕ the model predicts a first-order dependence of *L*, although the experimental results show indications of higher-order effects.

The model gives reasonable numerical agreement with the experiments, which suggests that the dominant physical processes are accounted for, in spite of the simplifying assumptions made. It is considered that in its current form the model allows useful predictions to be made that can act as a starting point for larger scale experimental trials.

References

- Ayel, V., Lottin, O., Peerhossaini, H., 2002. Rheology, flow behaviour and heat transfer of ice slurries: a review of the state of the art. Int. J. Refrigeration 26, 95–107.
- Bellas, I., Tassou, S.A., 2005. Present and future applications of ice slurries. Int. J. Refrigeration 28, 115–121.
- Bellas, J., Chaer, I., Tassou, S.A., 2002. Heat transfer and pressure drop of ice slurries in plate heat exchangers. Appl. Therm. Eng. 22, 721–732.
- Davies, T.W., 2005. Slurry ice as a heat transfer fluid with a large number of application domains. Int. J. Refrigeration 28, 108–114.
- Donev, A., Cisse, I., Sachs, D., Variano, E.A., Stillinger, F.H., Connelly, R., Torquato, S., Chaikin, P.M., 2004. Improving the density of jammed disordered packings using ellipsoids. Science 303 (5660), 990–993.
- Hansen, T.M., Rados.evic ´, M., Kauffeld, M., 2002. Behaviour of ice slurry in thermal storage systems. ASHRAE research project RP1166, Danish Technological Institute.
- Kauffeld, M., Kawaji, M., Egolf, P.W. (Eds.), 2005. Handbook on Ice Slurries: Fundamentals and Engineering. International Institute of Refrigeration, Paris.
- Metz, P., Margen, P., 1987. The feasibility and economics of slush ice district cooling systems. ASHRAE Trans. 93 (Part 2), 1672–1686.

- Mooney, M., 1951. The viscosity of a concentrated suspension of spherical particles. J. Colloid Sci. 6, 162–170.
- Niezgoda-Zelasko, B., 2006. Heat transfer of ice slurry flows in tubes. Int. J. Refrigeration 29, 437–450.
- Quarini, G.L., 2001. Cleaning and separation in conduits. Patent numbers GB2358229, WO0151224.
- Quarini, G.L., 2002. Ice-pigging to reduce and remove fouling and to achieve clean-in-place. Appl. Therm. Eng. 22, 747–753.
- Shire, S., Quarini, J., Ayala, R.S., 2005a. Ultrasonic detection of slurry ice flows. Proc. IMechE Part E: J. Process Mech. Eng. 219, 217–225.
- Shire, S., Quarini, J., Ayala, R.S., 2005b. Experimental investigation of the mixing behaviour of pumpable ice slurries and ice pigs in pipe flows. Proc. IMechE Part E: J. Process Mech. Eng. 219, 301–309.
- Shire, G.S.F., 2006. The behaviour of ice pigging slurries. Ph.D. thesis, University of Bristol.
- Sari, O., Vuarnoz, D., Meili, F., Egolf, P.W., 2000. Visualisation of ice slurries and ice slurry flows. In: Proceedings of the Second Workshop on Ice Slurries of the IIR, Paris, pp. 68–81.
- Stamatiou, E., Kawaji, M., Goldstein, V., 2002. Ice fraction measurements in ice slurry flow through a vertical rectangular channel heated from one side. In: Proceedings of
- the Fifth Workshop on Ice Slurries of the IIR, Stockholm, pp. 82–93.
- Wills, J.M., 1991. An ellipsoid packing in E^3 of unexpected high density. Mathematika 38, 318–320.